Mechanistic Studies of the Pyrolysis of 1,3-Butadiene, 1,3-Butadiene-1,1,4,4-d_4, 1,2-Butadiene, and 2-Butyne by Supersonic Jet/Photoionization Mass Spectrometry

Steven D. Chambreau,[†] Jessy Lemieux, Liming Wang,[‡] and Jingsong Zhang*[,§]

Department of Chemistry, University of California, Riverside, California 92521

Received: November 2, 2004; In Final Form: December 24, 2004

The thermal decomposition of 1,3-butadiene, 1,3-butadiene-1,1,4,4-d_4, 1,2-butadiene, and 2-butyne at temperatures up to 1520 K was carried out by flash pyrolysis on a ~20 μs time scale. The reaction products were isolated by supersonic expansion and detected by single-photon ($\lambda = 118$ nm) vacuum-ultraviolet time-of-flight mass spectrometry (VUV-TOFMS). Direct detection of CH_3 and C_3H_3, as well as C_3H_4, C_4H_4, and C_4H_5 products, provides insight into the initial steps involved in the complex pyrolysis of these C_4H_6 species below $T = 1500$ K. The similar pyrolysis product distributions for the C_4H_6 isomers on such a short time scale support the previously proposed mechanism of facile isomerization of these species. Isomerization of 1,3-butadiene to 1,2-butadiene and subsequent C−C bond fission of 1,2-butadiene to produce CH_3 and C_3H_3 (propargyl) are most likely the primary initial radical production channel in the 1,3-butadiene pyrolysis.

Introduction

To understand the mechanisms involved in soot formation in combustion, much work has been done on the thermal decomposition pathways of small hydrocarbons. Although the thermal decomposition of 1,3-butadiene (1,3-C_4H_6) has been studied extensively,[1−7] the details of the mechanism have continued to be a subject of debate. Of particular interest is the initiation of 1,3-butadiene pyrolysis. On the basis of entropic arguments, Keifer et al. proposed that the primary initiation step was the cleavage of the C−C bond to form two vinyl radicals.[2−4]

$$1,3\text{-}C_4H_6 \rightarrow 2C_2H_3 \quad (1)$$

However, the mechanism based on this initiation step did not accurately account for ethylene production. Skinner et al. and later Rao et al. suggested initiation by unimolecular decomposition to ethylene and acetylene.[5,6]

$$1,3\text{-}C_4H_6 \rightarrow C_2H_2 + C_2H_4 \quad (2)$$

Admittedly, some of the assumptions made were somewhat in disagreement with the known kinetic data.[1−6] Reaction 2 is currently believed to proceed through the short-lived vinylidene, $:CCH_2 \rightarrow C_2H_2$.[3] Similar to the fast isomerization between allene and propyne,[8] Kern et al.[9] and, more recently, Hidaka et al.[1,10] presented an alternative mechanism in which 1,3-butadiene first isomerized to 1,2-butadiene (1,2-C_4H_6) and 2-butyne (2-C_4H_6), forming terminal single C−C σ bonds:

$$1,3\text{-}C_4H_6 \rightarrow 1,2\text{-}C_4H_6 \quad (3)$$

$$1,3\text{-}C_4H_6 \rightarrow 2\text{-}C_4H_6 \quad (4)$$

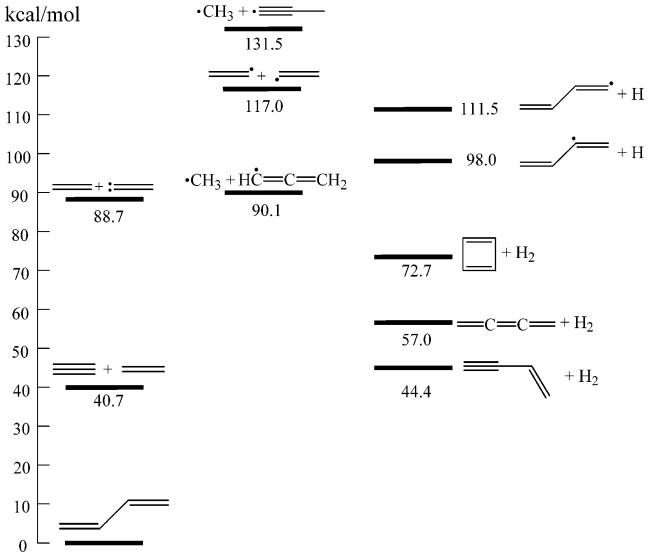

Figure 1. Relative energies of the species involved in the 1,3-butadiene pyrolysis, taken from refs 1 and 28 (the values were determined from heats of formation at 298 K).

1,2-Butadiene (or 2-butyne) then decomposed to CH_3 and C_3H_3 radicals that initiated subsequent radical chain processes:

$$1,2\text{-}C_4H_6 \rightarrow CH_3 + C_3H_3 \quad (5)$$

The isomerization of 1,3-C_4H_6 to 1,2-C_4H_6 and 2-C_4H_6 was shown to be much faster than its decomposition at high temperatures.[1] The introduction of this initiation mechanism to the previous reaction scheme resolved many of the differences between previous models and experimental data.[1]

In most of the previous studies, the thermal decomposition mechanisms of 1,3-butadiene were examined mainly by end products analysis. In this work, the extent to which each of the initiation steps (reactions 1−5 and Figure 1) occur is evaluated by direct observation of the initial pyrolysis products (especially free radicals) using flash pyrolysis (in tens of microseconds)

* Corresponding author. Fax: +1-951-827-4713. E-mail: jingsong.zhang@ucr.edu.

[†] Present address: Department of Chemistry, Wayne State University, Detroit, MI 48202.

[‡] Present address: Department of Chemistry, University of Leeds, Leeds LS2 9JT, UK.

[§] Also at Air Pollution Research Center, University of California, Riverside, CA 92521.

10.1021/jp045010r CCC: $30.25
Published on Web 02/15/2005

and time-of-flight mass spectrometry (TOFMS). The complication from subsequent chemical reactions is minimized. Quantum chemistry calculations of the energy barriers and transition state geometries for the isomerization reactions are carried out, and possible mechanisms are discussed and compared to current literature.

Experimental Section

The pyrolysis experiments were conducted on an apparatus that was previously described.[11−13] 1,3-Butadiene was obtained from Matheson (99.8%), 1,3-butadiene-1,1,4,4-d_4 (98%) was from Cambridge Isotope Laboratories, and 1,2-butadiene (99%) and 2-butyne (99%) were from Aldrich. 1,3-Butadiene and its d_4 species were diluted to ∼1% in helium and used without any further purification. 1,2-Butadiene and 2-butyne were introduced by bubbling He through the liquid or over the solid at reduced temperatures to control the vapor pressure. Bath temperatures for 1,2-butadiene and 2-butyne were ∼195 and 226 K, respectively. The concentrations for 1,2-butadiene and 2-butyne were <1%. The stagnation pressure of the gas mixtures was 130 kPa. The flash pyrolysis source was based on the design of Chen and co-workers.[14] Flash pyrolysis was achieved by expanding the gas mixtures through a heated SiC nozzle (Carborundum, heated length 10 mm, 2 mm o.d., 1 mm i.d.). The nozzle was heated resistively with the electrical current being controlled by a Variac transformer. The nozzle temperature was monitored by a type C (Omega) thermocouple attached to the outside of the nozzle that had previously been calibrated to the internal temperature of the nozzle. With a near sonic velocity of the sample within the nozzle, the residence time in the heater has been estimated to be approximately 20 μs.[14,15] After leaving the nozzle, products were cooled and isolated by supersonic expansion into vacuum where they proceeded to the photoionization region.

The parent molecules and products were ionized by 118 nm (10.48 eV) photons produced by frequency tripling the 355 nm output of a Nd:YAG laser in a Xe cell (∼20 Torr) and were subsequently detected by a linear time-of-flight mass spectrometer (R. M. Jordan Co.[16]). The 118 nm radiation was focused by a MgF_2 lens through a small aperture into the photoionization zone, while the fundamental 355 nm beam diverged in this region. This divergence and the aperture minimized multiphoton ionization (MPI) and the amount of scattered 355 radiation within the ionization region, which will be discussed below. The TOF spectra were collected using a digital oscilloscope (Tektronix TDS3032) and averaged over 512 laser shots; they were then converted to mass spectra using the appropriate Jacobian transformation.

The approaches in this experiment present several advantages: (1) a short reaction time to examine the initial steps of the thermal decomposition; (2) supersonic cooling, quenching the reaction and minimizing recombination of products and intermediates; and (3) minimal ion fragmentation by the use of the 10.48 eV "soft" photoionization source that imparts sufficient energy to ionize many closed-shell and free radical species. The supersonic cooling further reduces photoionization fragmentation by minimizing the internal energy of the parent molecules and the pyrolysis products.

The energetics for decompositions and isomerizations of the C_4H_6 species were calculated using quantum chemistry methods. The geometries were optimized using hybrid density functional method B3LYP with 6-31+G(2df,p) basis sets,[17,18] and the vibrational frequencies were calculated at the same level of theory for characterizing the nature of structures and computing zero-point energy corrections. Accurate energies were obtained

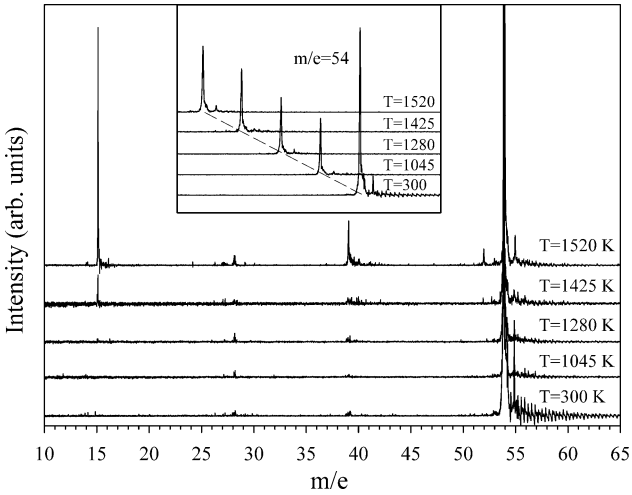

Figure 2. TOF mass spectra of flash pyrolysis of 1,3-butadiene (1% in He) with the nozzle temperatures between 300 and 1520 K using 10.48 eV photoionization. The mass spectra in the inset are in full scale and are offset in both mass and baseline for clarity.

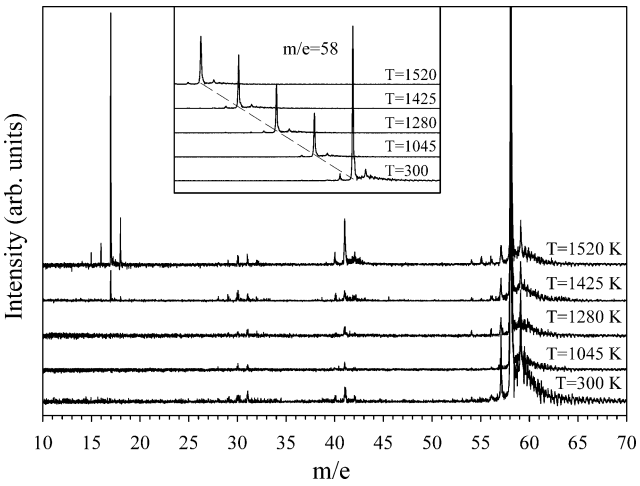

Figure 3. Mass spectra of flash pyrolysis of 1,3-butadiene-1,1,4,4-d_4 (1% in He) with the nozzle temperatures between 300 and 1520 K using 10.48 eV photoionization. The mass spectra in the inset are in full scale and are offset in both mass and baseline for clarity.

at the Gaussian 3X (G3X) level.[19−21] To compare with the available experimental values, the relative energies of species were listed on the basis of the enthalpies of formation at 0 K (see Figures 6 and 7), calculated from the G3X atomization energies. All transition states were confirmed by following the intrinsic reaction coordinates (IRCs) to the desired isomers. It was found that the IRCs from different levels of theory were very close; however, the saddle point along IRC may shift position when the level of theory changes. The "true" transition states were therefore located as the maximum from a high level of theory along the IRC from a relatively low-level theory. In the present study, the transition states were located at QCISD(T)/6-31G(d) level along the IRC at B3LYP/6-31+G(2df,p) level, IRC-Max((U)QCISD(T)/6-31G(d)//(U)B3LYP/6-31+G(2df,p)).[22] All ab initio and density functional theory calculations were performed using the Gaussian 98/03 suite of program.[23]

Results

1,3-Butadiene. The mass spectra of 1,3-butadiene are taken at 300 K and at pyrolysis temperatures of 1045, 1280, 1425, and 1520 K (Figure 2). At 300 K, a large 1,3-butadiene parent peak is observed at $m/e = 54$. Also present are very small peaks

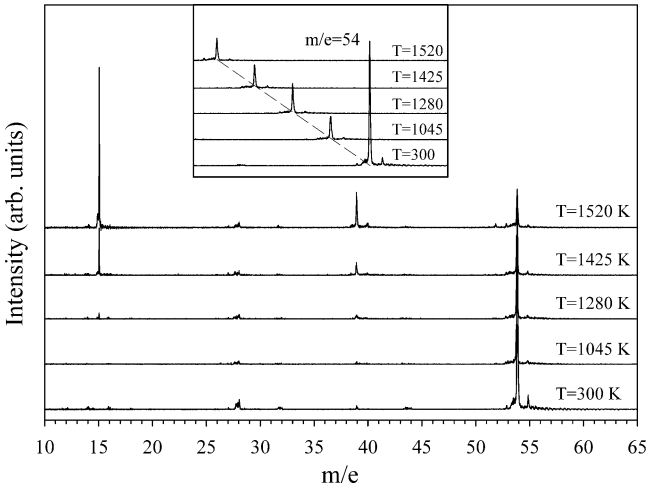

Figure 4. Mass spectra of flash pyrolysis of 1,2-butadiene (<1% in He) at the nozzle temperatures from 300 to 1520 K. The mass spectra in the inset are in full scale and offset in both mass and baseline.

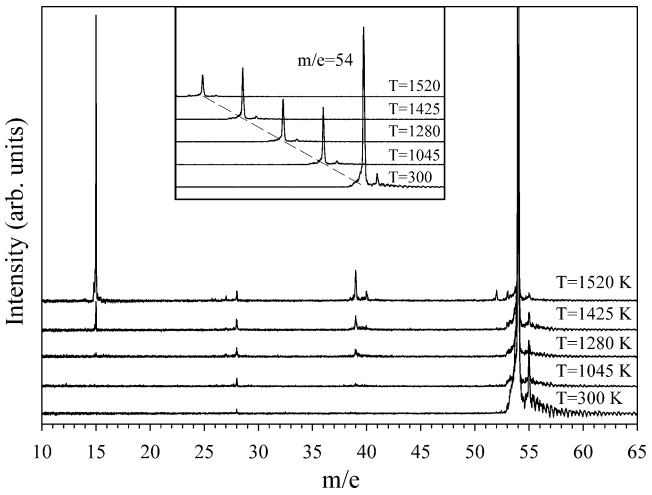

Figure 5. Mass spectra of flash pyrolysis of 2-butyne (<1% in He) at the nozzle temperatures from 300 to 1520 K. The mass spectra in the inset are in full scale and offset in both mass and baseline.

at $m/e = 28$ and 39 that correspond to C_2H_4 and C_3H_3, respectively. The appearance energies of $C_2H_4^+$ and $C_3H_3^+$ from 1,3-butadiene are 12.55 and 11.30 eV, respectively;[24] thus these species could not have been generated by the 10.48 eV photoionization source and are attributed to a small amount of electron impact ionization (EI, see the Discussion section for details).

For heater temperatures between 300 and 1280 K, with the exception of the $m/e = 54$ parent peak decreasing between 300 and 1045 K, all peak intensities remain relatively constant. At 1425 K, a distinct $m/e = 15$ methyl radical peak appears, and an $m/e = 39$ peak, corresponding to the C_3H_3 radical, begins to grow. At 1520 K, both $m/e = 15$ and $m/e = 39$ increase significantly. In addition, $m/e = 52-3$ peaks appear at 1425 K, and $m/e = 52$ grows significantly at 1520 K. Very small peaks at $m/e = 27$ and $m/e = 40$, corresponding to C_2H_3 and C_3H_4, are noticeable at 1520 K.

1,3-Butadiene-1,1,4,4-d_4. At 300 K, the mass peaks observed in 1,3-butadiene-1,1,4,4-d_4 are the large parent peak at $m/e = 58$, and smaller peaks at $m/e = 31$, 41, and 57 (Figure 3). The $m/e = 31$ peak corresponds to partially deuterated versions of ethylene, C_2D_3H. The $m/e = 41$ peak corresponds to C_3D_2H radical that is analogous to the C_3H_3 fragment found in the 1,3-butadiene room-temperature spectrum. The appearance energies are too high for these species to be produced by photoionization fragmentation at 10.48 eV. These minor peaks are the result of a small amount of EI. Smaller peaks are observed at $m/e = 29$, 30, 40, and 42. These satellites of the 31 and 41 peaks can be attributed to either rearrangement and subsequent fragmentation of the 1,3-butadiene-1,1,4,4-d_4 cation generated by EI, or possibly to impurities within the sample.

Upon the pyrolysis of 1,3-butadiene-1,1,4,4-d_4, the $m/e = 29-31$ and $40-42$ peaks maintain approximately the same size at 1045 and 1280 K. At 1280 K, additional peaks appear at $m/e = 54$ and 56. At 1425 K, a peak appears at $m/e = 17$, which corresponds to the deuterated methyl radical CD_2H. The $m/e = 17$ peak also has a small satellite at $m/e = 18$. Peaks at $m/e = 28-31$, $m/e = 40-42$, and $m/e = 55$ begin to grow at 1425 K. At 1520 K, there are large increases in the $m/e = 17$ and its satellites at $m/e = 15$, 16, and 18, as well as $m/e = 41$ peaks and its satellites, while the peaks at $m/e = 28-32$ increase slightly in size, as do $m/e = 54-6$.

1,2-Butadiene. The pyrolysis of 1,2-butadiene (see Figure 4) yields results similar to those of 1,3-butadiene (Figure 2). Small, constant peaks at $m/e = 28$ and $m/e = 39$, attributed to a small amount of EI, are observed at all temperatures. A CH_3 peak at $m/e = 15$ appears at 1280 K and increases at 1425 and 1520 K. A peak appears at $m/e = 39$ at 1280 K, which also increases as the temperature is raised to 1520 K. At 1520 K, a small peak appears at $m/e = 40$. Also observed at 1520 K are small $m/e = 52$ (C_4H_4) and 53 (C_4H_5) peaks due to loss of hydrogen by the parent.

2-Butyne. The pyrolysis of 2-butyne is also carried out with mass spectra being taken at 300, 1045, 1280, 1425, and 1520 K (Figure 5). At 300 K, the peaks present are the large parent peak at $m/e = 54$ and a small peak at $m/e = 28$, the latter resulting from ionization fragmentation due to EI. An $m/e = 39$ peak at 1280 K and an $m/e = 15$ peak at 1425 K appear due to C_3H_3 and CH_3 production, respectively, and whose intensities increase at 1520 K. Small peaks at $m/e = 52$ and 53 corresponding to C_4H_4 and C_4H_5 appear at 1520 K. An $m/e = 40$ peak also appears at 1425 K and grows at 1520 K. A small $m/e = 27$ peak appears at 1280 K and increases slightly at 1520 K.

Discussion

Electron Impact and Multiphoton Ionization. One limitation of this apparatus is the occurrence of a small amount of electron-impact ionization (EI) resulting from photoelectrons produced by scattered light within the photoionization region. Efforts were made to eliminate this effect, such as minimizing the 355 nm laser spot size with a telescope, and masking the photoionization region from the diverging 355 nm beam with an aperture. The attempts to eliminate all EI contributions resulted in the loss of the photoionization signal as well. A compromise was made to minimize the EI contribution while retaining sufficient photoionization signal. From the EI fragmentation pattern of 1,3-butadiene of Dannacher,[24] $m/e = 39$ has a 90% relative abundance as compared to the parent peak for EI with an electron energy of 75 eV. Based on this information and the intensity of the $m/e = 39$ peak at room temperature (Figure 2), EI contributions to the overall mass spectra in our experiment were estimated to be <1% of the overall signal. Fragmentation from EI should, in general, remain constant at all pyrolysis temperatures due to efficient supersonic cooling of the pyrolysis products, which has been observed in a previous experiment.[11]

The possibility of multiphoton ionization (MPI) occurring has also been considered. In the design of the 118 nm source, due

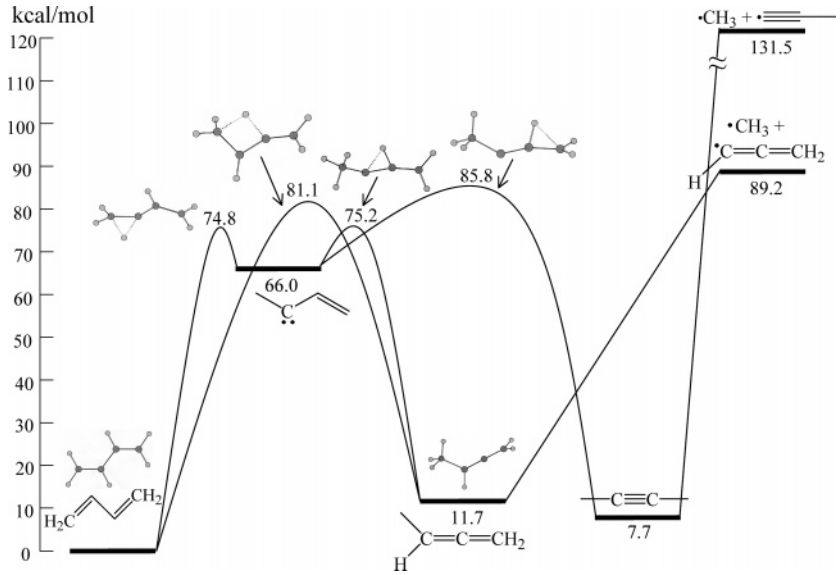

Figure 6. Energetics of H-shift isomerization of the C_4H_6 species via the methyl vinyl carbene intermediate in the butadiene pyrolysis. Enthalpies of formation of the stable species and transition state energies are calculated at the G3X level at 0 K and are used to determine the energetics. The $CCCH_3 + CH_3$ energy (298 K) is from ref 28.

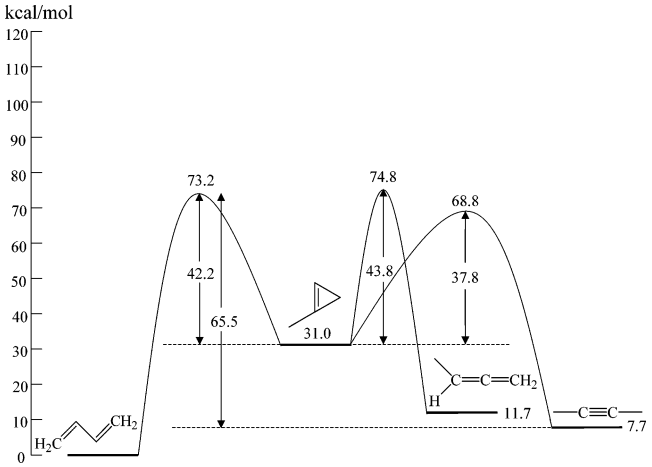

Figure 7. Energetics of isomerization of the C_4H_6 species via the 1-methylcyclopropene intermediate. Enthalpies of formation of the stable species are calculated at the G3X level at 0 K and are used to determine the energetics. Activation energies are experimental results of Hopf (at $T > 483$ K) from ref 31.

to the difference in the indices of refraction of the MgF_2 lens at 118 and 355 nm wavelengths, the 118 nm light is focused in the photoionization region, while the 355 nm light diverges here, minimizing multi-355 nm photon ionization. Indeed, without Xe, the tripling medium for VUV generation, no ion signals were observed for the butadiene pyrolysis at all temperatures, indicating negligible MPI (and EI) by the 355-nm fundamental UV radiation alone. MPI with 118 + 355 nm photons (14.0 eV) is also unlikely as indicated by the negligible fragmentation of the room-temperature mass spectrum of 1,3-butadiene (Figure 2). Photoionization fragmentation of 1,3-C_4H_6 at 14.0 eV would result in the formation of $m/e = 28$, 39, and 53 peaks, with appearance energies (EA) of 12.6, 11.3, and 11.4 eV, respectively,[24,25] and with $m/e = 39$ being the predominant fragment ion peak (comparable to the parent ion in peak intensity). The absence of a fragmentation $m/e = 39$ peak in the room-temperature spectrum of 1,3-C_4H_6 indicates the predominance of single 118-nm photon ionization, with negligible MPI and EI contributions to the spectra.

When C_2H_4 (IP = 10.51 eV) is leaked into the vacuum chamber at room temperature, it has sufficient internal energy (up to ~0.35 eV) to allow photoionization by the 118-nm VUV radiation at 10.48 eV, and a significant photoionization signal is recorded. However, the C_2H_4 after the supersonic expansion through the nozzle in the flash pyrolysis experiments yielded only a very small photoionization signal, and this small ion signal remained constant at all pyrolysis temperatures, again indicating efficient supersonic cooling and minimum photoionization fragmentation. Therefore, only the growth of mass peaks at elevated temperatures is considered indicative of the pyrolysis products.

Isomerization and C−C Bond Cleavage. The similarity of the pyrolysis mass spectra for each of the C_4H_6 isomers strongly suggests isomerization processes to a common species, followed by decomposition. The prevalence of the CH_3 and C_3H_3 species in the 1,3-C_4H_6 mass spectra at elevated temperatures indicates that the parent 1,3-C_4H_6 must isomerize so that a methyl group is terminal and that hydrogen migration occurs, possibly via multiple steps, before C−C bond cleavage. The likely species to dissociate to form CH_3 and C_3H_3 from a simple bond cleavage are 1,2-butadiene (1,2-C_4H_6), 1-butyne (1-C_4H_6), and 2-butyne (2-C_4H_6). Based on kinetic modeling, 1-C_4H_6 has been determined to be unimportant in the butadiene pyrolysis because of its slow isomerization rate to 1,3-C_4H_6,[1,26] which would be expected due to the complex, multistep mechanism of its formation from 1,3-C_4H_6.

Quantum mechanical calculations of energies and geometries of the C_4H_6 species and their transition states of isomerization, and heats of formation of CH_3 and C_3H_3, are performed to provide additional insight to help identify the lowest energy pathways involved in the butadiene pyrolysis (Figures 6 and 7). Based on the energetics, the energy threshold for $CH_3 + HCCCH_2$ (propargyl) production from 1,2-C_4H_6 is about 42 kcal/mol lower than that for $CH_3 + CCCH_3$ (propenyl) production from 2-C_4H_6, due to resonance stabilization of the propargyl radical (Figures 1 and 6). Recent 193 nm photodissociation/photoionization experiments of 1,3-C_4H_6 and 1,2-C_4H_6 by Robinson et al. confirm unambiguously that $HCCCH_2$ is produced and not $CCCH_3$.[27,28] It is interesting to note that, although the energies of the 193-nm photodissociation are substantially higher than the thermal energies of pyrolysis, the lower energy $HCCCH_2$ is nonetheless formed in the photodissociation of 1,3-C_4H_6 and 1,2-C_4H_6, presumably by internal

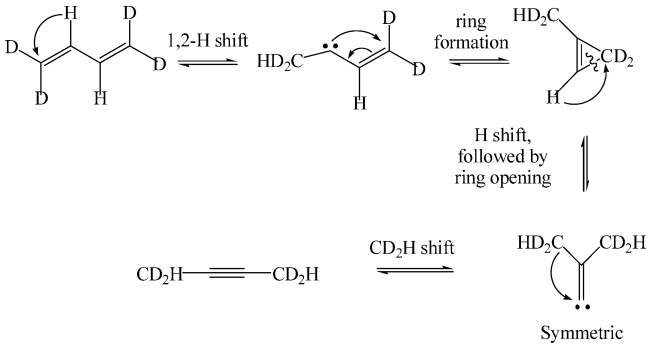

Figure 8. Mechanism for isomerization from 1,3-C_4H_6-1,1,4,4-d_4 to 2-C_4H_6-1,1,4,4-d_4 via the 1-methylcyclopropene intermediate. Note that the symmetric geometry of the alkylvinylidene intermediate prohibits H−D scrambling in this route.

conversion to the ground state, followed by unimolecular dissociation. Therefore, in the pyrolysis experiments of the C_4H_6 species, it is likely that 1,3-C_4H_6 and 2-C_4H_6 isomerize to 1,2-C_4H_6 first and then decompose into the $CH_3 + HCCCH_2$ (propargyl) products, the lowest-energy CH_3 elimination channel.

The isomerization from 1,3-C_4H_6 to 1,2-C_4H_6 could occur by a C2−C1 1,2-H shift to a methyl vinyl carbene intermediate[1,29,30] with a calculated barrier of 74.8 kcal/mol (in this study), followed by a C3−C2 1,2-H migration to form 1,2-C_4H_6, with a barrier for the reverse reaction of 63.5 kcal/mol (Figure 6). Our theoretical values of these two barrier heights are in agreement with the experimental values of 74.2 and 63.3 kcal/mol estimated by Hidaka et al.,[1,10] and they are also a good match to the recent G2M theoretical values of 73.9 and 62.8 kcal/mol, respectively, by Lee et al.[30] Another pathway for isomerization from 1,3-C_4H_6 to 1,2-C_4H_6 is the C3−C1 1,3-H shift to directly form 1,2-C_4H_6 (Figure 6). However, the calculated energy barrier is about 6 kcal/mol higher than that of the stepwise C2−C1 and C3−C2 1,2-H migration pathway; thus this channel is less likely to contribute to the 1,3-C_4H_6 to 1,2-C_4H_6 isomerization, except at higher temperatures. After isomerization from 1,3-C_4H_6 to 1,2-C_4H_6, 1,2-C_4H_6 readily decomposes to CH_3 and $HCCCH_2$.

The isomerization from 1,3-C_4H_6 to 2-C_4H_6 also requires multiple H shifts to occur. One possible pathway involves the formation of methyl vinyl carbene by the C2−C1 1,2-H shift, followed by a C3−C4 1,2-H shift, which has a barrier of 85.8 kcal/mol with respect to 1,3-C_4H_6 (calculated in this study, Figure 6) and is consistent with the 86.1 kcal/mol C3−C4 1,2-H shift barrier height estimated by Hidaka.[1] There is a lower energy pathway involving the formation of 1-methylcyclopropene via the methyl vinyl carbene, followed by an H shift and ring opening to form dimethylvinylidene, and subsequent methyl migration to form 2-C_4H_6 (Figures 7 and 8).[1,30−33] The overall barrier of 1,3-C_4H_6 to 1-methylcyclopropene is determined by the isomerization barrier of 1,3-C_4H_6 to methyl vinyl carbene, as the methyl vinyl carbene can readily isomerize to 1-methylcyclopropene via a lower barrier.[30,33,34] By combining the appropriate experimental activation energies of 1-methylcyclopropene isomerization by Hopf et al.[31] and the G3X theoretical heats of formation at 0 K (this study), the overall energy barrier for this first step (1,3-C_4H_6 to 1-methylcyclopropene via the methyl vinyl carbene) is estimated at 73.2 kcal/mol with respect to 1,3-C_4H_6 or 65.5 kcal/mol relative to 2-C_4H_6 (Figures 7 and 8),[31,32] which matches the isomerization barrier of 1,3-C_4H_6 to the methyl vinyl carbene, found to be 74.8 kcal/mol theoretically in this study (Figure 6). The second step is the isomerization of 1-methylcyclopropene to 2-C_4H_6 that involves an H shift and ring opening to form dimethylvinylidene, and subsequent methyl migration to form 2-C_4H_6 (Figure 8). The overall barrier of the second step is estimated to be 68.8 kcal/mol (relative to 1,3-C_4H_6) in this study (based on Hopf et al.'s activation energy), which is consistent with the barrier height of ∼70 kcal/mol (relative to 1,3-C_4H_6) by Hidaka et al.[1] and 68.4 kcal/mol by Lee et al.[30] Note that the overall barrier for the lower energy isomerization pathway from 1,3-C_4H_6 to 2-C_4H_6 via 1-methylcyclopropene is 73.2 kcal/mol relative to 1,3-C_4H_6 or 65.5 kcal/mol relative to 2-C_4H_6 (Figure 7), and this value is in agreement with the experimental activation energy of 65.0 kcal/mol for the reverse reaction 2-C_4H_6 → 1,3-C_4H_6 via the methyl migration.[34] The isomerization of 1,2-C_4H_6 to 1-methylcyclopropene is also via the methyl vinyl carbene intermediate, similar to that of 1,3-C_4H_6 to 1-methylcyclopropene;[30,33,34] and the overall barrier is determined by the 1,2-C_4H_6 to methyl vinyl carbene isomerization, which is calculated to be 75.2 kcal/mol (relative to 1,3-C_4H_6) in this study (Figure 6) and is estimated to be 74.8 kcal/mol (based on Hopf et al.'s activation energy, Figure 7). Note that in Figure 7 the isomerization of 1,3-C_4H_6 to 1,2-C_4H_6 is controlled by the methyl vinyl carbene intermediate and is essentially the same as the stepwise C2−C1 and C3−C2 1,2-H isomerization pathway from 1,3-C_4H_6 to 1,2-C_4H_6 in Figure 6. Thermal corrections at $T = 500$ K increase the heats of formation of all species in Figure 7 by 8−10 kcal/mol, and the energy barriers increase to 67.0, 69.6, and 75.6 kcal/mol for the 2-C_4H_6 to 1,3-C_4H_6, 1-methylcyclopropene to 2-C_4H_6, and 1-methylcyclopropene to 1,2-C_4H_6 routes, respectively. While these thermal corrections do shift the energy barriers slightly higher, the overall mechanistic implications remain the same. Finally, as the energy threshold for $CH_3 + HCCCH_2$ (propargyl) is ∼42 kcal/mol lower than that for $CH_3 + CCCH_3$ (propenyl) (Figure 6), it is likely that 2-C_4H_6 undergoes isomerization to 1,2-C_4H_6 via 1-methylcyclopropene (Figure 7), and then decomposes to $CH_3 + HCCCH_2$.

The pyrolysis mass spectra of 1,3-C_4H_6-1,1,4,4-d_4 could provide additional insights into the decomposition mechanisms of the C_4H_6 species. If the 2-C_4H_6-d_4 species formed by pyrolysis of 1,3-C_4H_6-1,1,4,4-d_4 through the 1-methylcyclopropene route decomposes to yield the deuterated equivalents of CH_3 and C_3H_3 radicals, the products would be exclusively CD_2H and C_3D_2H due to the symmetry of the dimethylvinylidene intermediate (Figure 8). The occurrence of H−D scrambling in 1,3-C_4H_6-1,1,4,4-d_4 pyrolysis indicates that the formation of the corresponding CH_3 and C_3H_3 species does not occur exclusively via the 1-methylcyclopropene intermediate route upon decomposition of 2-C_4H_6. In fact, the formation of $CH_3 + CCCH_3$ (propenyl) is unlikely due to the high energies involved, as stated previously. Instead, the formation of 1,2-butadiene by successive H shifts and C−C bond cleavage to form the corresponding CH_3 and $HCCCH_2$ (propargyl) species is the likely source of H−D scrambling (Figure 9). By comparing the peak heights of masses 16−18 in the spectra in Figure 3 (corrected for known impurities and ^{13}C contributions), the branching ratios for the various pathways in Figure 9 can be estimated. The branching ratios for CDH_2:CD_2H:CD_3 formation are 0:0.88:0.12 at 1425 K, and 0.06:0.79:0.15 at 1520 K. The predominance of CD_2H is due to requiring only two, lower energy barrier 1,2-H shifts (C2−C1 and C3−C2) to form 1,2-C_4H_6, while formation of CDH_2 and CD_3 requires three H(D) shifts (Figure 9), one possibly involving the higher energy barrier 1,3-H shift (see Figure 6).

The important features of the 1,3-butadiene pyrolysis in Figure 2, as well as those of 1,2-butadiene and 2-butyne, are

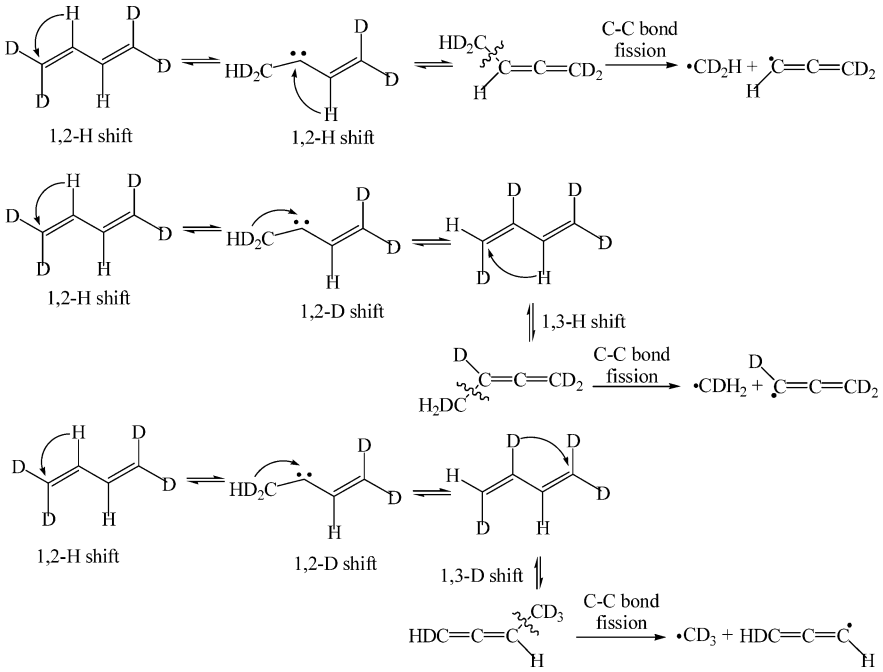

Figure 9. Possible routes for H−D scrambling in the isomerization of 1,3-C_4H_6-1,1,4,4-d_4 to 1,2-C_4H_6-d_4, with subsequent C−C bond cleavage.

the absence or very minor amount of C_2H_3 (m/e = 27 peak) detected and the prevalence of the CH_3 and C_3H_3 products. The near absence of C_2H_3 indicates that either it is not formed in significant amounts under our experimental conditions, it decomposes quickly to form C_2H_2 + H, or it has a small photoionization cross-section at 118 nm. Our prior experiment on nitroethylene pyrolysis and an early experiment by Chen and co-workers show that C_2H_3 radical can be readily detected by 118-nm photoionization TOFMS.[35] The recent determination of the absolute photoionization cross section of vinyl at 118 nm gives a value of 12.5 Mbarn,[36] versus 9.0 Mbarn for propargyl, the latter of which is easily detected by our photoionization technique. The absence or minor presence of the C_2H_3 radical product channel is most likely due to its higher energetics than that of the CH_3 and C_3H_3 channel (Figure 1). Indeed, in the conjugated system of 1,3-C_4H_6, the C2−C3 bond in 1,3-C_4H_6 (with a shorter C2−C3 bond length of 1.456 Å) is stronger than a typical C−C σ bond (with typical bond lengths of 1.54 and 1.35 Å for single and double C−C bonds); thus isomerization to 1,2-C_4H_6 and subsequent decomposition of its single C−C σ bond are energetically more favorable than the cleavage of the C2−C3 bond in 1,3-C_4H_6 (Figures 1 and 6).

It is difficult to evaluate in this experiment the significance of the ethylene and acetylene production channel, which was proposed by Rao et al.[6] and thought to be important by Tsang.[7] These species have ionization energies of 10.51 and 11.40 eV, respectively. Acetylene cannot be ionized by the 118-nm photoionization source, but some hot ethylene molecules may be ionized. Slight increases in the ethylene peaks at 1520 K in 1,3-C_4H_6 (Figure 2) indicate this molecular decomposition channel may also be present, but its significance cannot be quantified by our method due to the limited photoionization energy and the effective supersonic cooling of C_2H_4 mentioned previously.

C_4H_5 and C_4H_4 Production. The growth of the small peaks at m/e = 52 and 53 in the high-temperature pyrolysis of 1,3-butadiene, 1,2-butadiene, and 2-butyne indicates H loss reactions, either by direct C−H bond cleavage, H_2 elimination, or by H-abstraction reactions with the free radicals produced upon decomposition of the butadiene. The possible C−H bond dissociation channels of 1,3-C_4H_6 are shown in Figure 1: (i) H + n-C_4H_5 ($H_2CHCHCH$), with a dissociation energy of 111.6 kcal/mol calculated in this study; and (ii) H + i-C_4H_5 (H_2CHCCH_2), with a dissociation energy of 98.0 kcal/mol by the experiment,[1] 99.4 kcal/mol calculated in this study, and 98.8 kcal/mol by a recent calculation.[30] The H-atom loss channel of 1,2-C_4H_6 to form H + H_2CCCCH_3 requires 85.1 kcal/mol by the theory,[30] and that to form i-C_4H_5 requires 85.9 kcal/mol estimated by the experiment[10] and 86.9 kcal/mol by the theory.[30] The H-atom elimination channel of 2-C_4H_6 to form H + H_2CCCCH_3 requires 87.3 kcal/mol estimated by the experiment,[1] and 88.6 kcal/mol by the theory.[30] The energies for H elimination via C−H bond breaking from the various C_4H_6 isomers are at least 5 kcal/mol larger than those of their isomerization to 1,2-C_4H_6 followed by decomposition to CH_3 and C_3H_3, and thus the H loss channels by direct C−H bond cleavage should only compete with methyl loss channel (reaction 5) at high temperatures.

The appearance of the m/e = 52 peak at high temperatures indicates either loss of two H atoms or elimination of H_2 from the parent C_4H_6 molecules. The C_4H_5 species produced in the primary H loss processes mentioned above should not have enough internal energy to undergo secondary H elimination. However, if they suffer more collisions in the hot nozzle, they could further decompose to H + C_4H_4. For example, $H_2CCHCCH_2$ could decompose into the H + vinylacetylene products, via a barrier of ~45 and 43 kcal/mol endoergicity.[1,30] However, as the rates of the primary direct H loss from the C_4H_6 species are very small (due to the large C−H bond energies),[1] the contributions from this sequential H loss of C_4H_6 are limited. Molecular H_2 elimination of the C_4H_6 species leads to thermodynamically stable products such as vinylacetylene and butatriene (Figure 1). The activation energy of H_2 elimination from 1,3-C_4H_6 was estimated to be 94.7 kcal/mol.[1] A recent theoretical calculation indicates that the energy barrier for C2−C3 H_2 elimination from 1,3-C_4H_6 to form butatriene is 114.4 kcal/mol and the barrier for 1,1-H_2 elimination from 1,2-C_4H_6 to form vinylacetylene is 89.6 kcal/mol.[30] In addition, 1,3-C_4H_6 could undergo 1,1-H_2 elimination with a 96.0 kcal/mol barrier and a

86.1 kcal/mol endoergicity to form vinylvinylidene (which presumably will isomerize to vinylacetylene).[30]

Although the experimental conditions are designed to minimize reactive collisions following decomposition, the possibility of H-abstraction reactions cannot be ruled out. For example, the appearance of *m*/*e* 53 peak at high temperatures in Figure 2 could be consistent with the fast H-abstraction of 1,3-C_4H_6 by CH_3 and/or C_3H_3 (producing a small *m*/*e* 40 peak of C_3H_4):[1]

$$CH_3 + 1,3\text{-}C_4H_6 \rightarrow CH_4 + C_4H_5 \quad (6)$$

$$C_3H_3 + 1,3\text{-}C_4H_6 \rightarrow C_3H_4 + C_4H_5 \quad (7)$$

Reaction 6 has a preexponential factor A of $\sim 10^{14}$ cm^3 mol^{-1} s^{-1} and a modest activation energy E_a of 22.8 kcal/mol, while those of reaction 7 are $\sim 10^{13}$ cm^3 mol^{-1} s^{-1} and 22.5 kcal/mol, respectively. A simple kinetic modeling for the C_4H_6 species in ~ 20 μs reaction time indicates that the H-abstraction reaction by CH_3 and C_3H_3 could become significant above 1300 K, and the H-abstraction by CH_3 (such as reaction 6) is roughly 10 times more important than that by C_3H_3 (reaction 7). The C_4H_5 produced in the H-abstraction reactions could then undergo subsequent H elimination to form C_4H_4 at *m*/*e* 52 (such as vinylacetylene).[1] The rapid conversion of C_4H_5 to C_4H_4 might explain the peak height/product distribution difference between *m*/*e* = 53 and 52 in the pyrolysis mass spectra of 1,3-C_4H_6 in Figure 2. Indeed, the previous kinetic modeling results also confirm that the main pathway of C_4H_4 formation is via H-abstraction by CH_3 ($CH_3 + C_4H_6 \rightarrow CH_4 + C_4H_5$) and subsequent H loss ($C_4H_5 \rightarrow H + C_4H_4$).[1,10,34]

The high temperature profiles of the C_4H_6 parent mass peak seem to have a complex pattern. For example, the parent peaks of 1,3-C_4H_6 and 1,3-C_4H_6-1,1,4,4-d_4 increase slightly in the temperature range of 1045−1520 K, while those of 1,2-C_4H_6 and 2-C_4H_6 decrease or stay about the same. The previous kinetic modeling indicates that within the first 50 μs of pyrolysis reaction, the overall C_4H_6 number densities do not decrease drastically (by only about 20−30%) from 1100 to 1500 K,[1,10,34] consistent with the observations for 1,2-C_4H_6 and 2-C_4H_6 in this experiment. The small increase in the parent peaks of 1,3-C_4H_6 and 1,3-C_4H_6-d_4 with increasing temperature could be due to increased isomerization of 1,3-C_4H_6 to 1,2-C_4H_6 (which might have higher detection sensitivity in this experiment) or additional secondary reactions.

In summary, the proposed fast isomerization of the C_4H_6 species prior to C−C bond cleavage to form methyl and propargyl radicals has been confirmed by flash pyrolysis TOF mass spectrometry. Quantum chemistry calculations suggest a methyl vinyl carbene intermediate upon conversion from 1,3-C_4H_6 to 1,2-C_4H_6, while the formation of 1-methylcyclopropene is the likely intermediate in the 1,3-C_4H_6 to 2-C_4H_6 isomerization. After the isomerization of 1,3-C_4H_6 to 1,2-C_4H_6, 1,2-C_4H_6 could readily decompose to the methyl and propargyl radical products, and these radicals can then propagate additional free radical chain reactions.

Acknowledgment. This work was supported by the National Science Foundation (CHE-0111635 and CHE-0416244) and the Alfred P. Sloan Foundation. We thank Prof. Tom Morton for useful discussions.

References and Notes

(1) Hidaka, Y.; Higashihara, T.; Ninomiya, N.; Masaoka, H.; Nakamura, T.; Kawano, H. *Int. J. Chem. Kinet.* **1996**, *28*, 137.
(2) Kiefer, J. H.; Wei, H. C.; Kern, R. D.; Wu, C. H. *Int. J. Chem. Kinet.* **1985**, *17*, 225.
(3) Kiefer, J. H.; Mitchell, K. I.; Wei, H. C. *Int. J. Chem. Kinet.* **1988**, *20*, 787.
(4) Benson, S. W.; Haugen, G. R. *J. Phys. Chem.* **1967**, *71*, 1735.
(5) Skinner, G. B.; Sokolowski, E. M. *J. Phys. Chem.* **1960**, *64*, 1028.
(6) Rao, V. S.; Takeda, K.; Skinner, G. B. *Int. J. Chem. Kinet.* **1988**, *20*, 153.
(7) Tsang, W.; Mokrushin, V. *Proc. Combust. Institute* **2000**, *28*, 1717.
(8) Wu, C. H.; Kern, R. D. *J. Phys. Chem.* **1987**, *91*, 6291.
(9) Kern, R. D.; Singh, H. J.; Wu, C. H. *Int. J. Chem. Kinet.* **1988**, *20*, 731.
(10) Hidaka, Y.; Higashihara, T.; Ninomiya, N.; Oki, T.; Kawano, H. *Int. J. Chem. Kinet.* **1995**, *27*, 331.
(11) Chambreau, S. D.; Zhang, J.; Traeger, J. C.; Morton, T. H. *Int. J. Mass Spectrom.* **2000**, *199*, 17.
(12) Chambreau, S. D.; Zhang, J. *Chem. Phys. Lett.* **2001**, *343*, 482.
(13) Chambreau, S. D.; Zhang, J. *Chem. Phys. Lett.* **2002**, *351*, 171.
(14) Kohn, D. W.; Clauberg, H.; Chen, P. *Rev. Sci. Instrum.* **1992**, *63*, 4003.
(15) Friderichsen, A. V.; Radziszewski, J. G.; Nimlos, M. R.; Winter, P. R.; Dayton, D. C.; David, D. E.; Ellison, G. B. *J. Am. Chem. Soc.* **2001**, *123*, 1977.
(16) Lubman, D. M.; Jordan, R. M. *Rev. Sci. Instrum.* **1985**, *56*, 373.
(17) Lee, C.; Yang, W.; Parr, R. G. *Phys. Rev. B* **1988**, *37*, 785.
(18) Becke, A. D. *J. Chem. Phys.* **1993**, *98*, 5648.
(19) Curtiss, L. A.; Raghavachari, K.; Redfern, P. C.; Rassolov, V.; Pople, J. A. *J. Chem. Phys.* **1998**, *109*, 7764.
(20) Curtiss, L. A.; Redfern, P. C.; Rassolov, V.; Kedziora, G.; Pople, J. A. *J. Chem. Phys.* **2001**, *109*, 9287.
(21) Curtiss, L. A.; Redfern, P. C.; Raghavachari, K.; Pople, J. A. *J. Chem. Phys.* **2001**, *114*, 108.
(22) Malick, D. N.; Petersson, G. A.; Montgomery, J. A. *J. Chem. Phys.* **1998**, *108*, 5704.
(23) Frisch, M. J.; Trucks, G. W.; Schlegel, H. B.; Scuseria, G. E.; Robb, M. A.; Cheeseman, J. R.; Zakrzewski, V. G.; Montgomery, J. A.; Stratmann, R. E.; Burant, J. C.; Dapprich, S.; Millim, J. M.; Daniels, A. D.; Kudin, K. N.; Strain, M. C.; Farkas, O.; Tomasi, J.; Barone, V.; Cossi, M.; Cammi, R.; Mennucci, B.; Pomelli, C.; Adamo, C.; Clifford, S.; Ochterski, J.; Petersson, G. A.; Ayala, P. Y.; Cui, Q.; Morokuma, K.; Malick, D. K.; Rabuck, A. D.; Raghavachari, K.; Foresman, J. B.; Cioslowski, J.; Ortiz, J. V.; Stefanov, B. B.; Liu, G.; Liashenko, A.; Piskorz, P.; Komaromi, I.; Gomperts, R.; Martin, R. L.; Fox, D. J.; Keith, T.; Al-Laham, M. A.; Peng, C. Y.; Nanayakkara, A.; Gonzalez, C.; Challacombe, M.; Gill, P. M. W.; Johnson, B. G.; Chen, W.; Wong, M. W.; Andres, J. L.; Head-Gordon, M.; S., R. E.; Pople, J. A. *Gaussian 98/03*; Gaussian, Inc.: Pittsburgh, PA, 1998.
(24) Dannacher, J.; Flamme, J.; Stadelmann, J.; Voght, J. *Chem. Phys.* **1980**, *51*, 189.
(25) Sellers-Hahn, L.; Krailler, R. E.; Russell, D. H. *J. Chem. Phys.* **1988**, *89*, 889.
(26) Hidaka, Y.; Higashihara, T.; Oki, T.; Kawano, H. *Int. J. Chem. Kinet.* **1995**, *27*, 321.
(27) Robinson, J. C.; Sun, W.; Harris, S. A.; Qi, F.; Neumark, D. M. *J. Chem. Phys.* **2001**, *115*, 8359.
(28) Robinson, J. C.; Harris, S. A.; Sun, W.; Sveum, N. E.; Neumark, D. M. *J. Am. Chem. Soc.* **2001**, *124*, 10211.
(29) Evanseck, J. D.; Houk, K. N. *J. Phys. Chem.* **1990**, *94*, 5518.
(30) Lee, H.-Y.; Kislov, V. V.; Lin, S.-H.; Mebel, A. M.; Neumark, D. M. *Chem.-Eur. J.* **2003**, *9*, 726.
(31) Hopf, H.; Wachholz, G.; Walsh, R. *Chem. Ber.* **1985**, *118*, 3759.
(32) Graf von der Schulenburg, W.; Hopf, H.; Walsh, R. *Chem.-Eur. J.* **2000**, *6*, 1963.
(33) Yoshimine, M.; Pacansky, J.; Honjyou, N. *J. Am. Chem. Soc.* **1989**, *111*, 4198.
(34) Hidaka, Y.; Higashihara, T.; Ninomiya, N.; Oshita, H.; Kawano, H. *J. Phys. Chem.* **1993**, *97*, 10977.
(35) Blush, J. A.; Park, J.; Chen, P. *J. Am. Chem. Soc.* **1989**, *111*, 8951.
(36) Robinson, J. C.; Sveum, N. E.; Neumark, D. M. *J. Chem. Phys.* **2003**, *119*, 5311.